Composites: Part A 91 (2016) 388–397

Contents lists available at ScienceDirect

Composites: Part A

journal homepage: www.elsevier.com/locate/compositesa

Analysis of the Folgar & Tucker model for concentrated fibre suspensions in unconfined and confined shear flows via direct numerical simulation

R. Mezher [a], M. Perez [a], A. Scheuer [a,b], E. Abisset-Chavanne [a], F. Chinesta [a,*], R. Keunings [b]

[a] ICI - High Performance Computing Institute, Ecole Centrale de Nantes, 1 rue de la Noe, F-44300 Nantes, France
[b] ICTEAM, Université catholique de Louvain, Bat. Euler, Av. Georges Lemaitre 4, B-1348 Louvain-la-Neuve, Belgium

ARTICLE INFO

Article history:
Received 9 June 2016
Received in revised form 18 October 2016
Accepted 21 October 2016
Available online 25 October 2016

Keywords:
Concentrated fibre suspensions
Folgar & Tucker model
Fibre-fibre interactions
Direct numerical simulation
Confinement

ABSTRACT

The classical Jeffery model allows for the prediction of the flow-induced orientation in dilute fibre suspensions. In most industrial applications, however, fibre suspensions are concentrated and fibre-fibre interactions cannot be ignored any longer. These interactions have been traditionally modelled at the mesoscopic and macroscopic scales by introducing a phenomenological diffusion term inducing a randomizing effect. In the so-called Folgar & Tucker (F&T) model, widely used in applications, the diffusion coefficient is assumed to scale linearly with the flow intensity, the latter being described by the second invariant of the rate of strain tensor. Modifications and alternatives to the F&T model have been proposed in view of the difficulty for the F&T model to explain an apparent orientation delay observed experimentally in injection-moulded parts. The noticed deviations were attributed to the intense fibre-fibre interactions, thus pointing to the limitations of a phenomenological diffusion term for describing them. In the present work, we revisit the F&T model and compare its predictions with those obtained bysimplified yet state-of-the-art direct numerical simulation (DNS) in unconfined and confined simple shear flows for a range of shear rates and concentrations, the latter ensuring intense fibre-fibre interactions. In unconfined flows, we find that the F&T model agrees quantitatively with the DNS results once an adequate closure relation is considered for approximating the fourth-order orientation tensor involved in the F&T model. Thus, the results seem to confirm, at least in simple shear flows, the F&T assumption for the form of the isotropic rotary diffusion function scaling linearly with the magnitude of the scalar rate of deformation. Also, a linear scalingof the diffusivity with the fibre concentration is observed. This conclusion remains unexpectedly valid under moderately-confined flow conditions as soon as an advanced fitted closure, like the IBOF, is considered within the F&T model. Other simpler closures (e.g. quadratic or hybrid), however, definitively fail to address confinement issues as also reported in our former work for the dilute regime. Obviously, these conclusions rest on the validity of the considered state-of-the-art DNS, which remains at present an open question.

1. Introduction

As discussed in [2], the multiscale modelling of suspensions involving rods involves nine conceptual bricks, the first three concerning the microscopic scale, the next three the mesoscopic scale, and finally the last three the macroscopic scale. At each scale, the first brick deals with the definition of conformation variables able to describe the relevant physics; the second concerns the equation describing their evolution, and finally the third one addresses their contribution to the stress tensor, and thus to the suspension's rheology.

The microscopic scale describes the evolution of each individual particle, e.g. each rod in the case of fibre suspensions, through its orientation vector **p**. Even though it could be considered too coarse from the point of view of the finer scales of ab initio or molecular dynamics simulations, it currently constitutes the finest scale of representation in practical applications. This scale allows us to account explicitly for fibre-fibre interactions by considering both lubrication and contact forces, and then quantifying interaction effects on the suspension kinematics and more precisely on the orientation state. A full direct numerical simulation – DNS – can be envisaged at the microscopic scale, but the difficulty of solving

* Corresponding author.
E-mail addresses: Rabih.Mezher@ec-nantes.fr (R. Mezher), Marta.Perez-Miguel@ec-nantes.fr (M. Perez), Adrien.Scheuer@ec-nantes.fr, Adrien.Scheuer@uclouvain.be (A. Scheuer), Emmanuelle.Abisset-chavanne@ec-nantes.fr (E. Abisset-Chavanne), Francisco.Chinesta@ec-nantes.fr (F. Chinesta), Roland.Keunings@uclouvain.be (R. Keunings).

http://dx.doi.org/10.1016/j.compositesa.2016.10.023
1359-835X/

the Stokes flow problem for describing the fluid-fibre interactions and the flow-induced fibre orientation, as well as the excessive computational complexity that it involves, limits the practical use of this approach to the analysis of a small number of suspended particles, as considered in [20].To our knowledge, there is nowadays no simulation at that scale able to address many particles scenarios involving intense hydrodynamic and contact interactions. The use of few particles does not allow one to recreate the right representative volume element to conclude about the impact of particles on the kinematics of the fluid-particles ensemble. Such a simulation, with the required number of particles for ensuring the required amount of interactions, is currently unfeasible. Thus, in the present paper, we adopt a simplified yet state-of-the-art DNS, a coarse grained formulation, successfully used in [9,18,19,25,26,30,31,35], wherein it is assumed that fluid-fibre interactions are governed by hydrodynamic and contact forces that lead in absence of fibre-fibre interactions to the classical Jeffery model for dilute suspensions [28]. Although the presence of fibres is expected to alter the microscopic flow kinematics in highly concentrated suspensions, the simplified approach to DNS neglects this effect while addressing in a sophisticated way fibre-fibre interactions via the modelling of lubrication and contact forces. Simulations involving thousands of suspended fibres can thus be performed to study fibre-fibre interactions in some detail.

The above modelling approach is unable to address applications of industrial interest as it remains limited in practice to several thousands of fibres. For this reason, microscopic models are usually coarsened by introducing as a suitable microstructural descriptor the probability distribution function – pdf – $\Psi(\mathbf{x}, t, \mathbf{p})$, which gives the fraction of fibres that at position $\mathbf{x}$ and time t are oriented in direction $\mathbf{p}$. The equation governing the evolution of the pdf is the so-called Fokker-Planck equation, that must be solved in both physical and conformation spaces. This mesoscopic approach is a reasonable compromise between the detailed microscale modelling and the coarser macroscopic approach discussed below. Its main limitations are twofold: (i) the high-dimensional nature of the Fokker-Planck equation, which limits the use of mesh-based discretization techniques [11,32–34] and requires specific numerical strategies based on the use of particles [1,6,10,12–14] or separated representations within the PGD framework [7,8,15,16]; and (ii) the difficulty of accounting for fibre-fibre interactions. The latter can only be modelled phenomenologically at this level of description.

To account for fibre-fibre interactions, Folgar & Tucker [24] thus added a phenomenological diffusion term to the Fokker-Planck equation. The rotary diffusion coefficient is assumed to scale with the flow intensity, quantified by the second invariant of the rate of strain tensor. Once coarsened to the macroscopic scale (see below), this leads to the so-called Folgar & Tucker (F&T) model. For addressing anomalous experimental orientation findings at odds with F&T predictions, in particular a delay in the orientation rates, other models of fibre-fibre interactions have been proposed [22,23,37,39,40]. In these studies, the observed delay was attributed to the intense fibre-fibre interactions and modelled either with a modified diffusion term, a microscopic description of interactions, or by introducing a sliding mechanism between fibres and fluid. In [36], we revisited this issue and attributed the anomalous behaviour to the confinement effects discussed later in the present paper.

Numerical simulations of industrial forming processes call for mascroscopic models. These can obtained from a mesoscopic description in the form of an evolution equation for the so-called orientation tensors [3,4], i.e. the moments of the pdf $\Psi(\mathbf{x}, t, \mathbf{p})$. The main price to pay in this approach is the use of closure approximations and their possibly significant impact on the model predictions. In particular, closure relations are needed to express the fourth-order moment of the pdf as a function of the second-order moment. Several closure relations have been proposed [5,21,17,29,38], but no universally-valid solution exists.

In the context of fibre suspensions, the macroscopic model is the most widely used. It assimilates fibres to ellipsoids, considers as macroscopic descriptor the second-order orientation tensor $\mathbf{a}(\mathbf{x}, t)$ defined by

$$\mathbf{a}(\mathbf{x}, t) = \int_{\mathcal{S}} \mathbf{p} \otimes \mathbf{p}\ \Psi(\mathbf{x}, t, \mathbf{p})\ d\mathbf{p}, \tag{1}$$

where $\mathcal{S}$ is the surface of the unit sphere and it uses the Jeffery equation [28] for modelling the ellipsoid kinematics

$$\dot{\mathbf{p}} = \boldsymbol{\Omega} \cdot \mathbf{p} + \lambda(\mathbf{D} \cdot \mathbf{p} - \mathbf{D} : (\mathbf{p} \otimes \mathbf{p})\mathbf{p}). \tag{2}$$

Here, $\nabla\mathbf{v}$ is the velocity gradient, $\mathbf{D}$ and $\boldsymbol{\Omega}$ are the rate of strain and vorticity tensors respectively, $2\mathbf{D} = \nabla\mathbf{v} + (\nabla\mathbf{v})^T$ and $2\boldsymbol{\Omega} = \nabla\mathbf{v} - (\nabla\mathbf{v})^T$, and the shape factor λ depends on the ellipsoid aspect ratio r, $\lambda = \frac{r^2-1}{r^2+1}$.

The macroscopic F&T model is an evolution equation for the orientation tensor $\mathbf{a}$, that results from taking the time derivative of Eq. (1), substituting the Jeffery rotary velocity (2) and considering a randomizing term to account for fibre-fibre interactions:

$$\dot{\mathbf{a}} = \boldsymbol{\Omega} \cdot \mathbf{a} - \mathbf{a} \cdot \boldsymbol{\Omega} + \lambda\Big(\mathbf{D} \cdot \mathbf{a} + \mathbf{a} \cdot \mathbf{D} - 2\mathbf{A}^{clr} : \mathbf{D}\Big) - 6D_r\left(\mathbf{a} - \frac{\mathbf{I}}{3}\right), \tag{3}$$

where $\mathbf{I}$ is the unit tensor and the diffusion coefficient D_r is assumed to scale with the flow intensity, i.e.

$$D_r = C_I\dot{\gamma}, \tag{4}$$

where C_I is the so-called interaction coefficient, and $\dot{\gamma}$ is the second invariant of the rate of strain, that is $\dot{\gamma} = \sqrt{2\mathbf{D} : \mathbf{D}}$

For the typical fibres considered in the present work, assumed in the sequel as elongated ellipsoids with $r = 20$, we have $\lambda \approx 1$ so that Eq. (3) reduces to

$$\dot{\mathbf{a}} = \nabla\mathbf{v} \cdot \mathbf{a} + \mathbf{a} \cdot (\nabla\mathbf{v})^T - 2\mathbf{A}^{clr} : \mathbf{D} - 6D_r\left(\mathbf{a} - \frac{\mathbf{I}}{3}\right). \tag{5}$$

The symbol $\mathbf{A}^{clr}$ denotes a suitable closure relation that gives the fourth-order moment $\mathbf{A}$ of the pdf in terms of the second-order tensor $\mathbf{a}$.

The main aim of the present paper is to validate the F&T model by means of DNS simulations of shear flows in both unconfined and confined conditions. In the next section, we revisit the main ingredients of DNS that account for fibre-fibre interactions and thus allow us to address the concentrated regime. In Section 3, we analyse the effect of these interactions on the orientation rate in the unconfined flow regime. In Section 4, we establish the dependencies of the diffusion parameter of the F&T model on the effective rate of strain and the fibre concentration. Finally, we perform in Section 5 a similar analysis under confined flow conditions.

2. Direct numerical simulation

In this section, we revisit the main ingredients of the direct numerical simulation technique – DNS – developed in [35]. It is based on a number of simplifying assumptions, the most important ones being: (i) the regime is concentrated enough for ensuring numerous lubrication and contact interactions; (ii) the suspending fluid is Newtonian and incompressible; (iii) the flow is laminar; (iv) the velocity gradient is constant in the considered representative volume containing the population of fibres; (v) the fluid velocity is unperturbed by the presence and orientation of the fibres immersed in it; (vi) the mass of the fibres is negligible and inertial effects can be ignored; (vii) fibres are considered as rigid prolate

spheroids; (viii) interactions between fibres act through contact and lubrication forces, (ix) initially and before the flow starts, the fibres are randomly distributed inside the representative volume with the only constraint of avoiding interpenetration, and (x) the initial orientation state is almost isotropic.

As described in [35], the flow applies on each fibre an hydrodynamic force (Stokes drag) that, in absence of interaction forces, implies that the fibre centre of gravity moves with the local fluid velocity and that the fibre rotates as dictated by Jeffery's model.

When fibre-fibre interactions occur, the fibre kinematics are modified. Two kinds of interactions are considered: (i) the one associated to lubrication whose intensity scales with both the distance between interacting fibres and with its rate of change, and (ii) the one related to physical contact that ensures impenetrability. Interaction forces act on a pair of interacting fibres at their contact point, with the same intensity but opposite directions (according to the Newton's law). At present, friction forces at the contact point are neglected, and contact forces are thus perpendicular to the involved fibres.

As described and discussed in [35], two fibres are assumed to interact as soon as the distance between them becomes lower than a small-enough threshold value. The simulation time step decreases with decreasing threshold. In our simulations, the threshold distance is specified as 0.01 times the fibre diameter, as proposed in [9]. In all cases, convergence was checked with respect to the number of fibres and the choice of threshold distance.

The approach rate between interacting fibres can be computed from the velocity of their respective centres of gravity and their rotary velocities, both consisting of the Jeffery contributions complemented by the contributions due to interaction forces. Thus, we obtain a linear system of equations from which all interaction forces can be determined, and from them their contributions to the fibre kinematics. Finally, the centre of gravity position and the orientation of each fibre are updated. For more details, the interested reader can refer to [35] and the references therein.

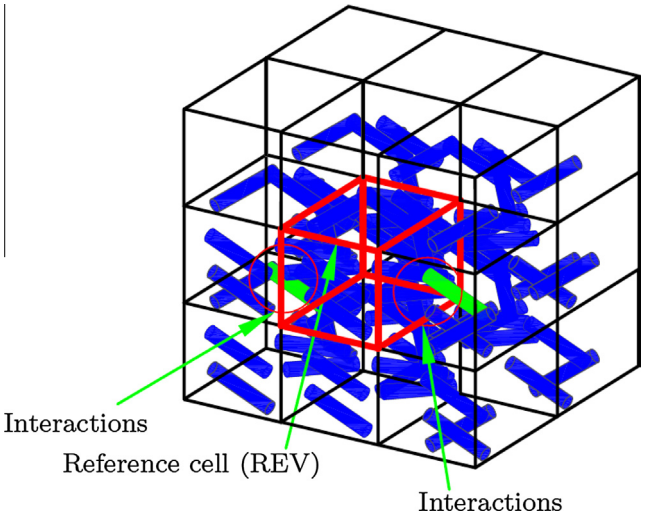

Fig. 1. Representative volume. Even though the fibres are depicted here as cylinders, they are considered as elongated ellipsoids in the models and DNS studies. (For interpretation of the references to color in this figure legend, the reader is referred to the web version of this article.)

The discrete simulation is performed in a representative elementary volume – REV – containing both fibres and fluid, as depicted in Fig. 1. The REV is then replicated in order to ensure periodic conditions. Thus, the motion of a fibre in the original REV implies the same motion of its images in the neighbouring cells, a fibre leaving the REV results in one of its images entering it. Moreover, we assume that each fibre within the REV interacts with its neighbouring fibres within the REV or in each of the neighbouring cells. Once the position and orientation of each fibre within the REV is updated, it is replicated in all neighbouring cells.

3. Orientation rate in concentrated unconfined flows

We consider a monodisperse population of fibres characterised by the parameters given in Table 1. Here, L is the fibre length, D its diameter, ϕ the fibre concentration, $N_I(t=0)$ the initial number of interactions between fibres, and N_F the total number of fibres. Two different cases are considered, which only differ in the initial number of fibre interactions, 500 and 800 respectively. A simple shear flow of intensity $\dot{\gamma}$ is applied, with a velocity field given by $\mathbf{v}^T = (\dot{\gamma}y, 0, 0)$.

Once the simulation has started, the centre of gravity position $\mathbf{X}_i^n$ and orientation $\mathbf{p}_i^n$ of each fibre $i = 1, \ldots, N_F$ are updated at each time step $t_n = n\Delta t$, according to the procedure summarised in the previous section.

From this information, the second-order orientation tensor $\mathbf{a}^{DNS}(t_n)$ can be computed at time t_n via its discrete definition

$$\mathbf{a}^{DNS}(t_n) = \frac{1}{N_F}\sum_{i=1}^{N_F} \mathbf{p}_i^n \otimes \mathbf{p}_i^n. \tag{6}$$

It is expected, and numerically observed, that fibres tend to almost align along the flow direction. In view of fibre-fibre interactions, however, full alignment is impossible and a quasi-steady orientation $\mathbf{a}_\infty^{DNS} = \mathbf{a}^{DNS}(t \to \infty)$ is reached instead.

We now consider the F&T model (5). It is an evolution equation for the second-order orientation tensor $\mathbf{a}$ whose single adjustable parameter, i.e. the diffusion coefficient D_r, will be computed such as to almost reach the same steady state $\mathbf{a}^{F\&T}(t \to \infty) \approx \mathbf{a}_\infty^{DNS}$ as predicted by DNS. It is important to note that the fitted value of D_r depends on the closure relation adopted in Eq. (5). In order to minimise the impact of the closure relation, we consider a quite robust and accurate closure, the IBOF [17], because the hybrid closure tends to overestimate in shear flows both the orientation rate and its long-time value. Moreover, the IBOF was itself originally fitted by considering, among many flow regimes, simple shear flows like the one addressed here, so that it is expected to have a minimal impact on the computed results. Once the diffusion coefficient has thus been fitted, both transient solutions $\mathbf{a}^{DNS}(t)$ and $\mathbf{a}^{F\&T}(t)$ can be compared in order to conclude on the ability of the F&T model to describe the orientation evolution when intense fibre-fibre interactions occur.

For the first scenario of Table 1, the fitted diffusion coefficient was found to be $D_r = 0.00015$. The corresponding time evolution of the components $\mathbf{a}_{ij}$ of the orientation tensor computed from DNS and the integration of the F&T model (5) are compared in

Table 1
Simulated scenarios.

Case	L (in mm)	D (in mm)	ϕ (in %)	$N_I(t=0)$	$\dot{\gamma}$ (s^{-1})	N_F
1	20	1	11.5	500	1	512
2	20	1	11.5	800	1	512

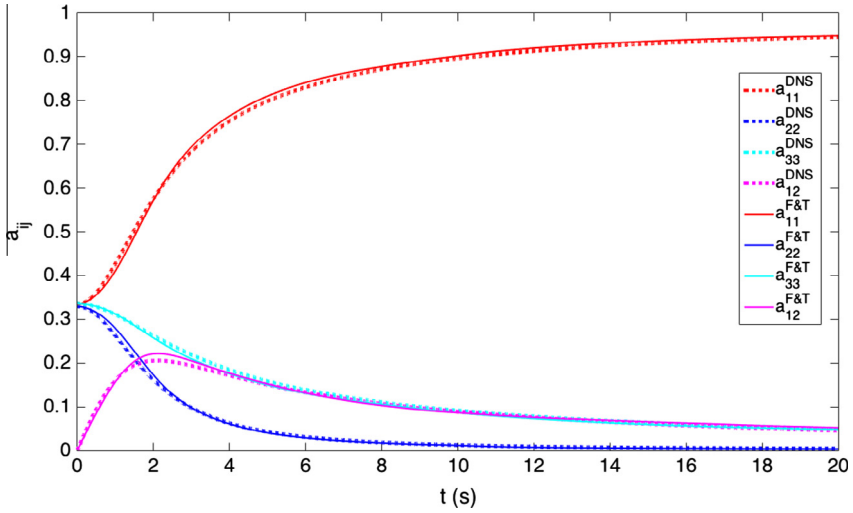

Fig. 2. Comparing $\mathbf{a}_{ij}^{DNS}(t)$ and $\mathbf{a}_{ij}^{F\&T}(t)$ for $N_I(t=0)=500$. (For interpretation of the references to color in this figure legend, the reader is referred to the web version of this article.)

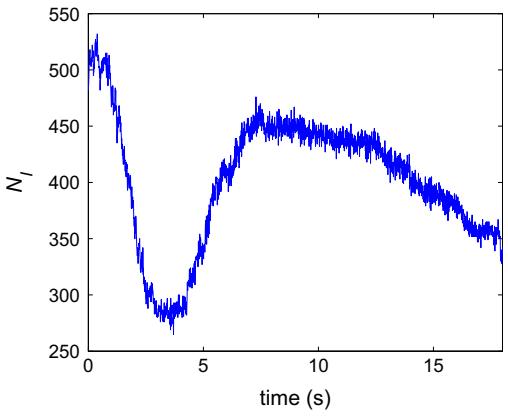

Fig. 3. Time evolution of the number of interactions for $N_I(t=0)=500$. (For interpretation of the references to color in this figure legend, the reader is referred to the web version of this article.)

Fig. 2 (components $\mathbf{a}_{13}$ and $\mathbf{a}_{23}$ almost vanish and are thus not shown). Fig. 3 depicts the time evolution of the number $N_I(t)$ of fibre-fibre interactions. Agreement between DNS and the F&T model is striking in view of the phenomenological description of fibre-fibre interactions that the latter provides.

The second scenario of Table 1 was considered to study the effect of increasing the number of fibre-fibre interactions. For that purpose, when introducing randomly a fibre, if it does not interact with any of its neighbours, the fibre is ignored and another tentative fibre is randomly created. If in one of the trials the test fibre interacts with one of its neighbours, it is retained and the algorithm goes to the next one. We defined a limit number of trials $\mathcal{T}$, such that if during $\mathcal{T}$ consecutive trials no interaction is found, the fibre is added to the REV and the algorithm proceeds to search for the next one. By changing the limit number of trials $\mathcal{T}$, one can modify the initial number of interactions. In the cases shown in Table 1, $\mathcal{T}$ was respectively 6 and 12. When increasing the number of initial fibre-fibre interactions, from 500 to 800 (second scenario in Table 1), and without changing the previously-fitted diffusion coefficient in the F&T model, the solution was mostly the same as that obtained in the first case with 500 initial fibre-fibre interactions. Moreover, the time evolution of the number of interactions is in both cases almost the same, independently of the initial value: a decrease at first, followed by a slight overshootas shown in Fig. 3, before almost reaching a steady-state plateau when an essentially steady-state orientation is established, shown and discussed in [35].

From the DNS results, we can notice a quite high long-time value of the orientation $\mathbf{a}_{11}(t\to\infty)\approx 0.95$ characteristic of semi-dilute suspensions, even if the concentration and fibre aspect-ratio clearly indicate a concentrated regime (in the confined case discussed in the last section, the long-time orientation mostly agrees with the expected values of alignment). The explanation for this apparently too high value of the long-time orientation lies in the fact that when applying an unconfined shear flow the particles try to almost align in the flow direction, and consequently the number and intensity of the fibre interactions decrease (as discussed in [35]). Thus, even if the considered concentrations clearly indicate that we are operating in the concentrated regime, the long-time solution implies about one interaction on average per fibre, which for the concentrations and particle aspect ratios considered here characterises the semi-concentrated regime. The type of regime depends on the concentration, on the particle aspect ratio but also on the flow-induced conformation. In all cases, it is important to recall that we neglect the incidence of the particle orientation on the microscopic flow kinematics (i.e. on the local fluid velocity at each point of the RVE),and then, as indicated in the abstract, these conclusions rest on the validity of the state-of-the-art DNS considered here, that future works, operating at the real DNS scale by solving the Stokes equations while accounting for the rich inter-particle interactions, should confirm.

We carried out a final DNS in which fibres do not interact with their neighbouring particles, and then each of them follows the kinematics dictated by the Jeffery equation. It was found that the solution remains very close to the one obtained when considering interactions, the main difference being found at long-times when the Jeffery solution tends to full alignment whereas the one including interactions reaches a plateau. In the simulation time window of 20 s depicted in Fig. 2, both solutions are indiscernible, and it was at later times that the solution of the Jeffery model continues to approach full alignment characterised by $\mathbf{a}_{11}^{Jef}\approx 1$ whereas the one related to the DNS incorporating fibre-fibre interactions reaches the plateau $\mathbf{a}_{11}^{DNS}\approx 0.95$.

From these numerical experiments, we conclude that the diffusion term in the F&T model mimics reasonably well the physics of fibre-fibre interactions in the concentrated shear flow regimeobtained from the simplified DNS described in the previous section.

4. On the dependencies of the F&T diffusion coefficient

In this section, we analyse the evolution of the F&T diffusion coefficient D_r with the shear rate and the fibre concentration. In fact, the F&T model assumes a linear dependence of D_r on $\dot{\gamma}$, which we wish to check via DNS. For that purpose, 9 simulations have been performed, whose conditions are reported in Table 2. The fibre population is once again monodisperse with $L = 20$ and $D = 1$.

Table 2
Simulation scenarios for different values of shear rate, fibre concentration and fitted diffusion coefficient.

Case	$\dot{\gamma}$ (s^{-1})	ϕ (in %)	N_f	D_r
1	1	7	512	0.00007
2	10	7	512	0.0007
3	20	7	512	0.0014
4	1	10	729	0.0001
5	10	10	729	0.001
6	20	10	729	0.002
7	1	18.2	1331	0.0002
8	10	18.2	1331	0.0018
9	20	18.2	1331	0.004

From an almost isotropic fibre orientation at the initial time $t = 0$, the shear flow is applied and DNS simulations are carried out. The orientation tensor is obtained at each time step as explained in the previous section and the diffusion coefficient involved in the F&T equation is obtained such as one approaches as much as possible the long-time solution of the different components of the orientation tensor(all components are considered with the same weights in the inverse technique). Table 2 reports in its last column the fitted diffusion coefficient. Fig. 4 depicts the evolution of the diffusion coefficient with shear rate for different fibre concentrations, as well as its evolution with concentration for different shear rates. We observe an almost linear dependence on both parameters, at least within the considered intervals of shear rate and concentrations. A non-linear dependence of the diffusion coefficient was observed experimentally [27] at much larger concentrations (higher than 33%) in experiments emulating compression moulding of SMC's. Future works should address larger intervals.

The resulting orientation evolutions are depicted in Fig. 5 for the different cases. It was observed that DNS predicts the same long-time orientation independently of the applied shear rate. In order to remove the influence of the shear rate in the steady-state solution of the Folgar & Tucker model (5), it suffices to

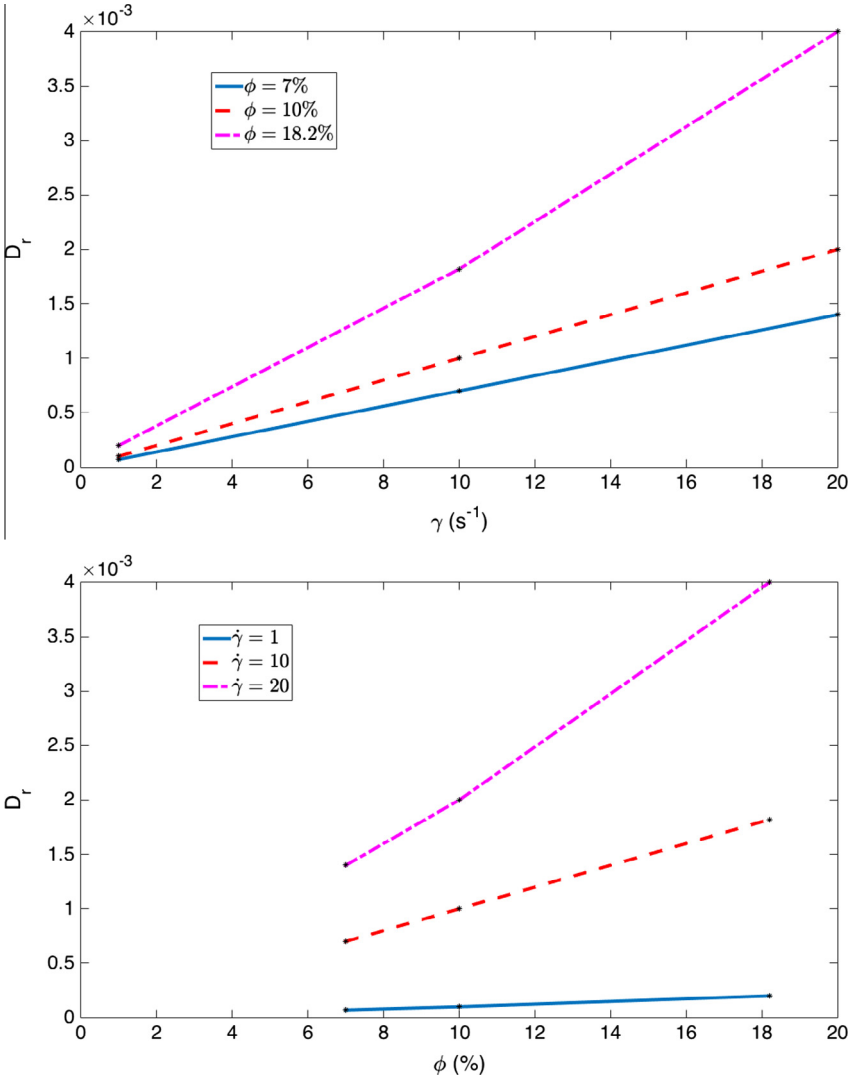

Fig. 4. Evolution of D_r with (top) $\dot{\gamma}$ at different fibre concentrations; and (bottom) with ϕ at different shear rates. (For interpretation of the references to color in this figure legend, the reader is referred to the web version of this article.)

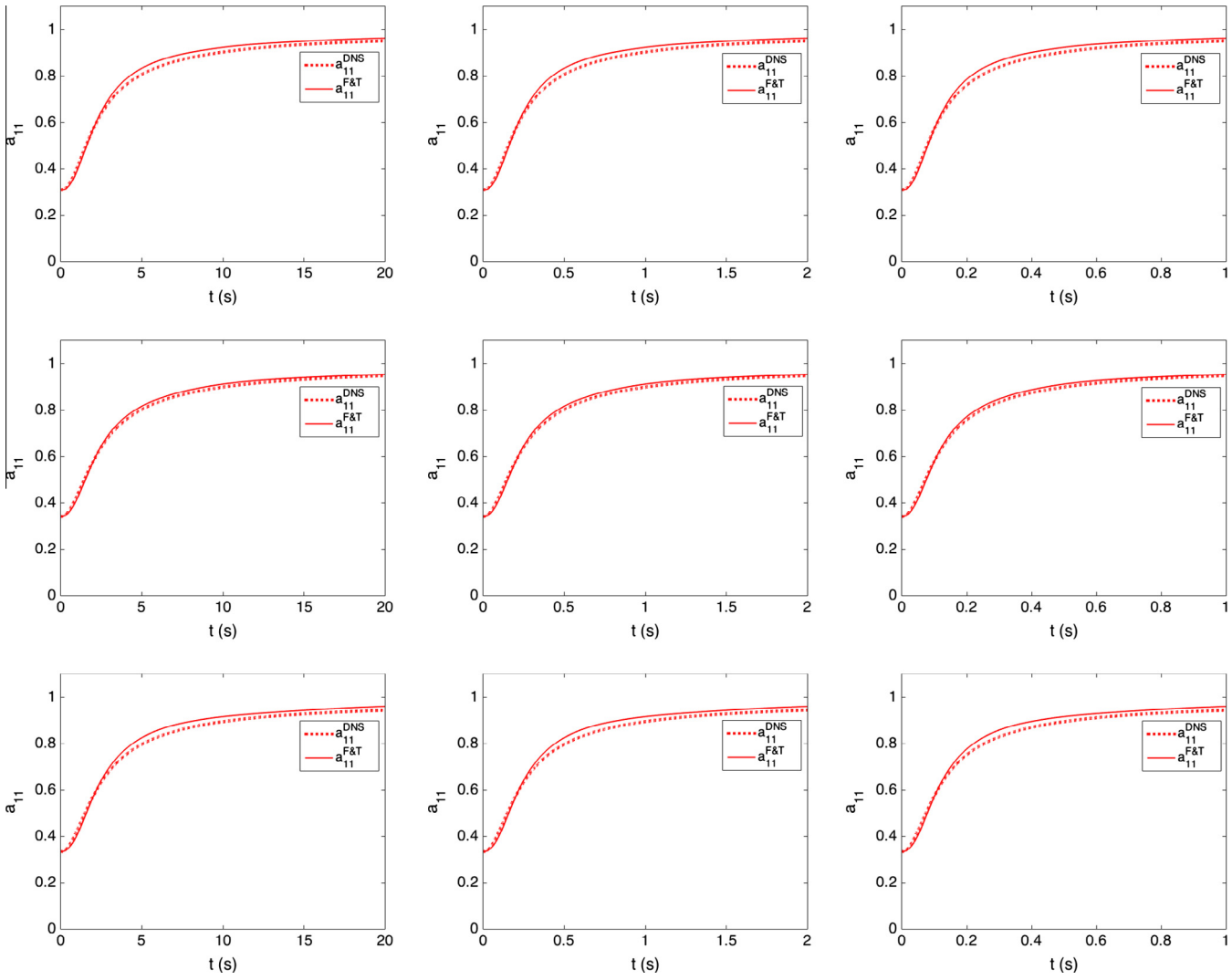

Fig. 5. Time evolution of a_{11}: (top-left) $\dot{\gamma} = 1, \phi = 7\%$ and $D_r = 0.00007$; (top-centre) $\dot{\gamma} = 10; \phi = 7\%$ and $D_r = 0.0007$; (top-right) $\dot{\gamma} = 20; \phi = 7\%$ and $D_r = 0.0014$; (middle-left) $\dot{\gamma} = 1; \phi = 10\%$ and $D_r = 0.0001$; (middle-centre) $\dot{\gamma} = 10; \phi = 10\%$ and $D_r = 0.001$; (middle-right) $\dot{\gamma} = 20; \phi = 10\%$ and $D_r = 0.002$; (bottom-left) $\dot{\gamma} = 1; \phi = 18\%$ and $D_r = 0.0002$; (bottom-centre) $\dot{\gamma} = 10; \phi = 18\%$ and $D_r = 0.0018$ and (bottom-right) $\dot{\gamma} = 20; \phi = 18\%$; and $D_r = 0.004$. (For interpretation of the references to color in this figure legend, the reader is referred to the web version of this article.)

consider a diffusion coefficient evolving linearly with the shear rate. Thus, the long-time orientation resulting from the integration of the Folgar & Tucker model does not depend on the applied shear rate. A deeper question is whether such a linear dependence is a necessary consequence. Of course, in absence of interactions, everything scales linearly with the shear rate, however as soon as non-linear interaction effects are present, a linear scaling is not at all obvious.

5. Confinement effects

From the previous results, it cannot be concluded that the experimentally-reported delay in the orientation process is due to the fibre-fibre interactions occurring in the concentrated regime. In this section, we evaluate the potential impact of confinement effects, which we studied in [36] in the dilute regime, where the effects of the almost planar orientation distribution were emphasised.

The main conclusions reached in [36] are that the orientation process is not delayed by confinement effects and that the second-order orientation tensor associated to a standard hybrid closure is no longer an adequate miscrostructural descriptor under highly confined conditions. We wish to find out whether or not those conclusions, valid for the dilute regime, extend to the concentrated regime wherein intense fibre-fibre interactions occur, as well as to analyse the effect of using the IBOF closure considered above in the analysis of unconfined flows.

We considered as in the previous section a population composed of 512 fibres confined in a narrow gap of 12 mm, smaller that the fibre length (20 mm) to ensure confinement effects. It is important to note that the gap-thickness to fibre-length ratio, $H/L = 0.6$, is larger than the values (of about 0.2) associated to the strong confinement considered in [36]. Thus, the first conclusions of the present section only apply for moderately-confined flow regimes, while more intense confinement will be addressed at the end.

In the present case, the RVE remains periodic along the x and y directions, however along the z direction the top and bottom walls enforce a null normal velocity at the particle/wall contact point. A simple shear flow ($\mathbf{v} = (\dot{\gamma}z, 0, 0)^T$) with $\dot{\gamma} = 1\ \mathrm{s}^{-1}$ was specified for the direct numerical simulation. When a fibre enters in contact with the upper or bottom wall, an additional contact force acts in order to ensure the wall impenetrability. The discrete orientation is calculated again at each time step, and the diffusion coefficient

in the F&T model (5) is fitted in order to reach the same long-time solution ($D_r = 0.006$ when using the IBOF closure). It is important to note that, when comparing results for the confined and unconfined flow regimes (the latter was considered in the previous section), a higher diffusion coefficient was needed in the confined case since the long-time solution (orientation plateau) is less aligned along the flow direction than in the unconfined case.

Fig. 6 depicts the almost steady-state fibre orientation distribution related to the initial orientation state depicted in Fig. 7. Here, the fibre concentration is set to $\phi = 11.5\%$. It can be noticed that the orientation evolves towards an orientation state with fibres almost oriented in the flow direction. Fig. 8 compares the evolution of the number of fibre-fibre and fibre-wall interactions. Fibre-fibre interactions are found to be much more numerous than fibre-wall interactions.

We compare in Fig. 9 the time evolution of the diagonal components of the second-order orientation tensor computed with DNS with that predicted by the F&T model (5) when using the IBOF closure relation with $D_r = 0.006$ (the non-diagonal components are almost zero). Fig. 10 compares the F&T solution $\mathbf{a}_{11}$ for three different closure relations: the quadratic, the hybrid and the IBOF. The F&T diffusion coefficient associated to each closure was again fitted to reach the same long-time solution (as indicated above, $D_r = 0.006$ for the IBOF and $D_r = 0.025$ for the quadratic and hybrid closures), and we specified as initial orientation tensor the one related to the initial orientation distribution shown in Fig. 7. We observe from both figures, 9 and 10, that the orientation process predicted by the F&T model (5) when considering the quadratic and hybrid closure relations is significantly faster than the DNS predictions. We thus reach the same conclusion as in our former work [36] for the dilute regime: under confined conditions and considering the standard hybrid closure within the F&T model, the only use of the second-order tensor cannot adequately predict the orientation development(when including the fourth and sixth-order orientation tensors, the solutions are not much improved). However, the combination of the Folgar & Tucker model (5) with the IBOF closure relation allows for an excellent prediction of the moderately-confined results obtained by using DNS. This fact suggests that the time evolution of the orientation distribution function in the moderately-confinement addressed here remains close enough to those that served to fit the IBOF closure relation, thusevidencing once again its superiority with respect to the simpler, non-fitted closures.

It is useful to compare the above results for the concentrated regime to those obtained when fibre-fibre interactions are ignored altogether. Fig. 10 also shows the predictions for the same fibre population wherein each individual fibre now obeys the confined Jeffery kinematics detailed in [36] for the dilute case. Thus, only fibre-wall interactions are taken into account and the orientation tensor is computed directly from a ensemble average of the form (6). Comparing with the DNS results for the concentrated regime, we see that the effect of intense fibre-fibre interactions remains quite moderate and only induces a very slight delay with respect to the dilute-regime predictions of the discrete confined Jeffery

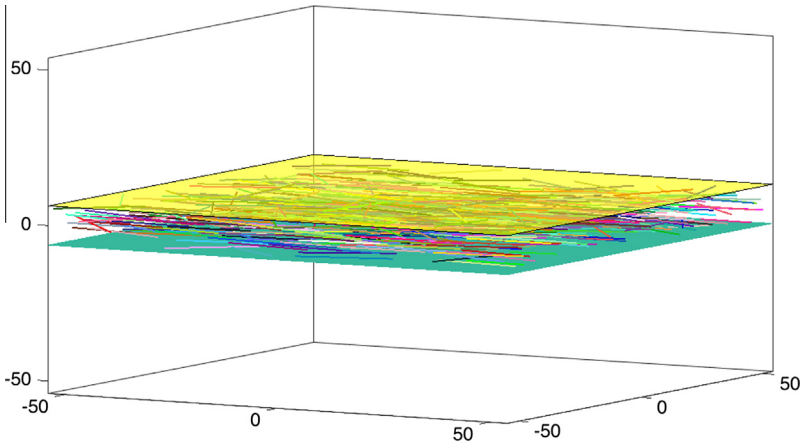

Fig. 6. Almost steady-state orientation distribution related to the initial fibre distribution depicted in Fig. 7. (For interpretation of the references to color in this figure legend, the reader is referred to the web version of this article.)

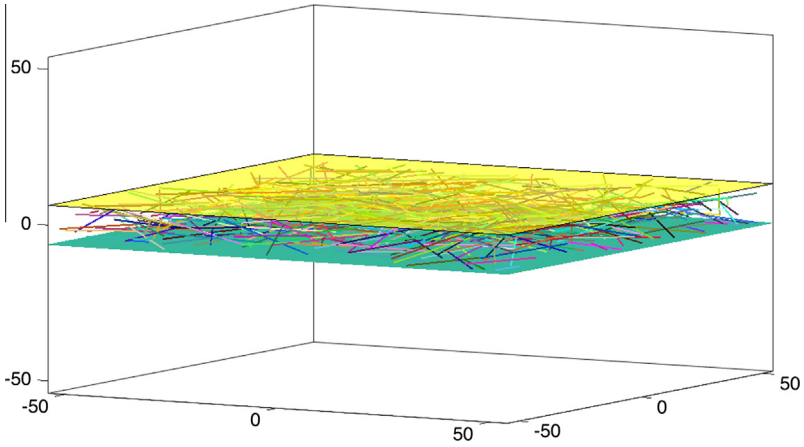

Fig. 7. Initial orientation distribution. (For interpretation of the references to color in this figure legend, the reader is referred to the web version of this article.)

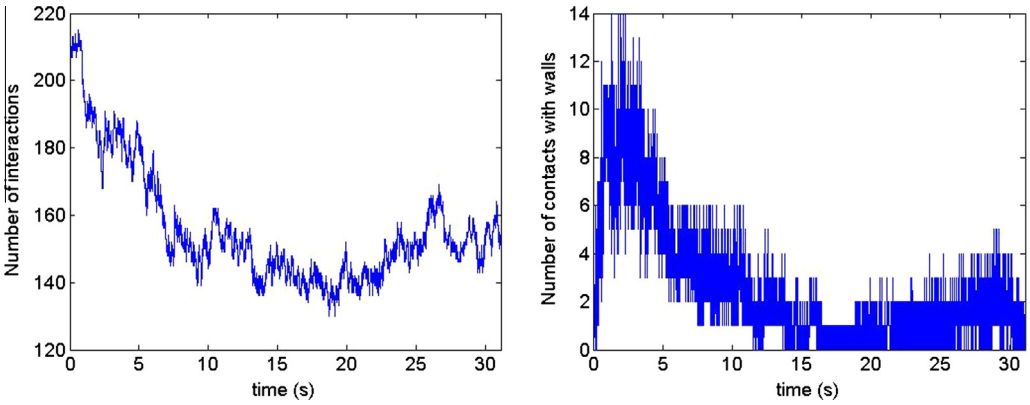

Fig. 8. Number of interactions: (left) fibre-fibre and (right) fibre-wall. (For interpretation of the references to color in this figure legend, the reader is referred to the web version of this article.)

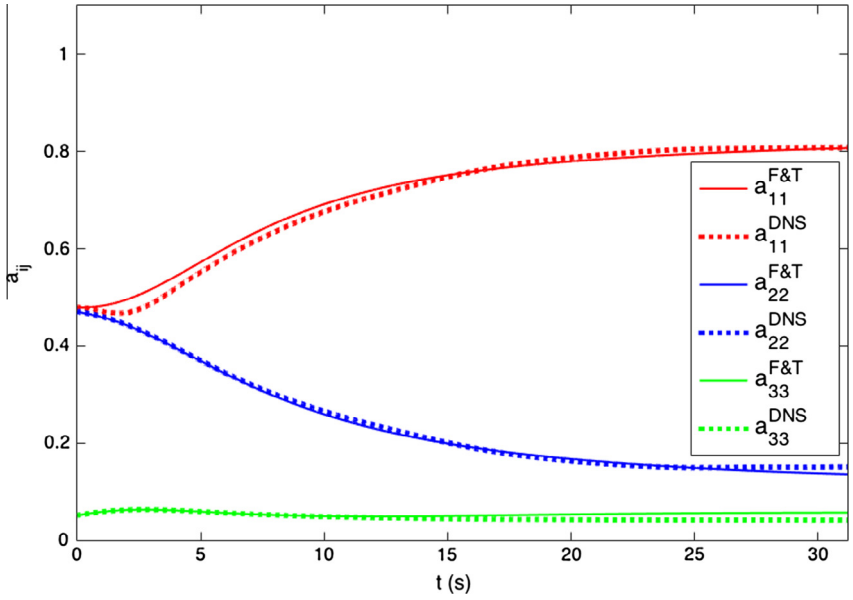

Fig. 9. Time evolution of the diagonal components of the orientation tensor in a confined shear flow: DNS versus F&T solution making use of the IBOF closure relation. (For interpretation of the references to color in this figure legend, the reader is referred to the web version of this article.)

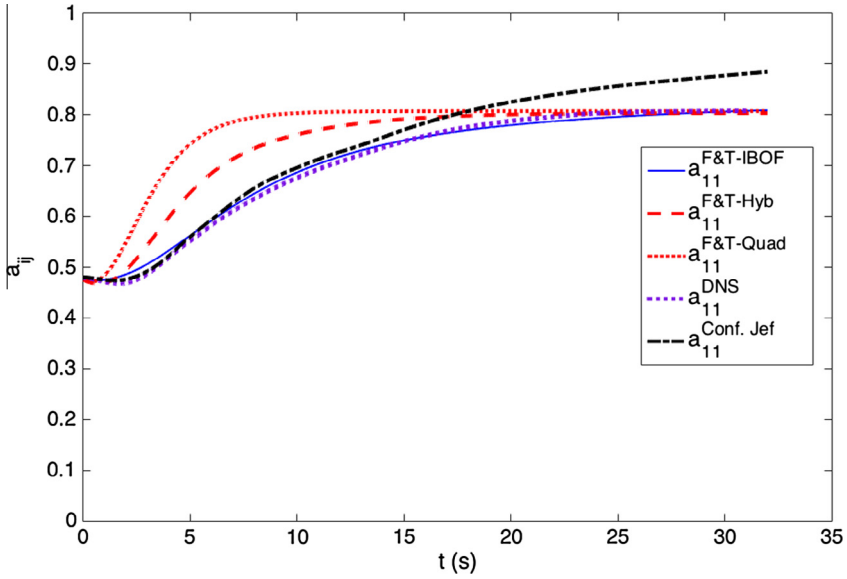

Fig. 10. Time evolution of the orientation tensor component $\mathbf{a}_{11}$ in a confined shear flow related to the F&T solutions for three different closure relations: quadratic, hybrid and IBOF, as well as for the confined Jeffery solution that ignores fibre-fibre interactions. (For interpretation of the references to color in this figure legend, the reader is referred to the web version of this article.)

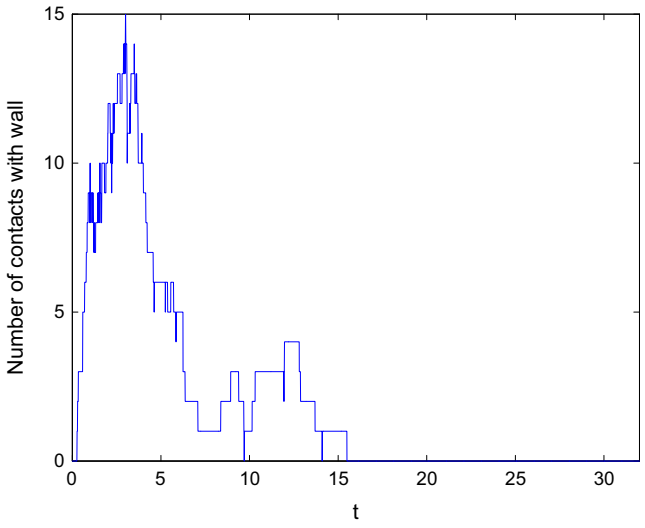

Fig. 11. Number of fibre-wall interactions predicted by the confined Jeffery model (fibre-fibre interactions are ignored). (For interpretation of the references to color in this figure legend, the reader is referred to the web version of this article.)

model(that ignores fibre-fibre interactions). While the confined Jeffery and DNS results almost match at the beginning of the orientation process, the former tend towards full alignement in the flow direction while the latter reach an orientation plateau in view of fibre-fibre interactions. Finally, Fig. 11 shows the evolution of the number of fibre-wall interactions predicted by the discrete confined Jeffery simulation. It is quite similar to that predicted by DNS for the concentrated regime (Fig. 8).

We carried out a final numerical experiment by solving the F&T model with null diffusion (dilute regime) and using the IBOF closure relation, and compared the results with the reference solution given in Fig. 11 of [36] where confinement is stronger $H/L = 0.2$. For the sake of completeness, this result is depicted in Fig. 12 where the discrete confined, the discrete unconfined and the solution related to the IBOF closure are compared and significant deviations are noticed. In this comparison, significant differences were noticed, which proves that the IBOF closure seems to be quite robust and accurate but is far from being a universal solution.In fact, we can only ensure that IBOF performs well within the conditions that served to fit it.

In summary, confinement effects limit the validity of the use of the second-order orientation tensor as microstructure descriptor. In the confined regime,the quadratic and hybrid closures fail when used within the F&T model. In the case of moderately-confined flows, the IBOF closure within the F&T framework agrees quite well with DNS. However, by increasing the confinement intensity $H/L \approx 0.2$, and even in absence of interactions (confined Jeffery's discrete solution versus F&T solution – with $D_r = 0$ – making use of the IBOF closure, that agree perfectly in the unconfined regime), both solutions differ significantly.

In those strongly-confined situations, and as concluded in our former work [36], two routes can be followed: (i) use of a set of microstructure descriptors richer than the single second-order orientation tensor, or (ii) look for better closure relations involving the second-order moment only that could be fitted in confined flow conditions, following the same rationale that was considered for deriving the IBOF closure in [17].

6. Conclusions

In this paper, the orientation kinematics of concentrated fibre suspensions have been revisited by comparing, in the case of unconfined and confined shear flows, direct numerical simulation results with predictions of the Folgar and Tucker macroscopic model (5) wherein fibre-fibre interactions are accounted for via a phenomenological randomizing diffusion term.

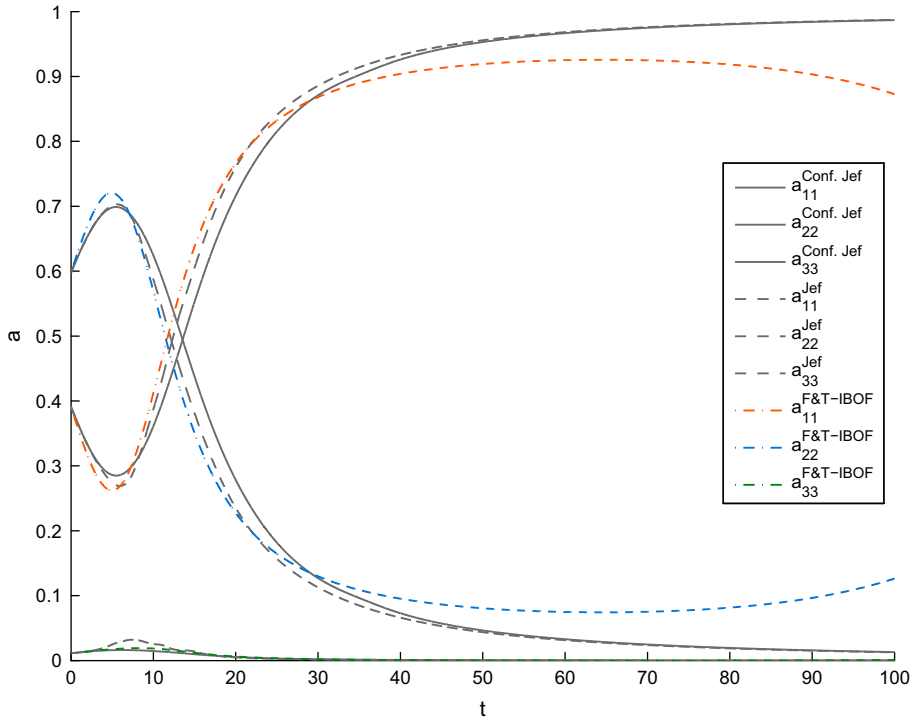

Fig. 12. Comparing the discrete confined, the discrete unconfined and the solution related to the IBOF closure. (For interpretation of the references to color in this figure legend, the reader is referred to the web version of this article.)

In the case of unconfined shear flow, we find that the F&T model combined with the IBOF closure captures the orientation evolution very well despite the occurrence of numerous fibre-fibre interactions in the concentrated regime. Our DNS results also show that in that case the F&T diffusion coefficient in simple shear flows scales linearly with the effective rate of strain as well as with the fibre concentration, at least within the explored intervals.

Under moderately-confined flow conditions and whenusing the quadratic or hybrid closures, the F&T model shows noticeable deviations from the direct numerical simulation results. This is in agreement with our former work [36] for the dilute regime (no fibre-fibre interactions), where the inability of the second-order orientation tensor combined withthe quadratic or hybrid closures to describe confined orientation states was pointed out. However, the F&T model combined with the IBOF closure captures the orientation evolution in the concentrated and moderately-confined flow regime.When comparing results for the confined and unconfined flow regimes, a higher diffusion coefficient was needed in the confined case. In the case of strongly-confined flows, no available closure relation seems appropriate for describing the orientation evolution with the F&T model.

The results of the present paper combined with those for the dilute regime [36] show that fibre-fibre interactions and confinement only have a very slight effect on the orientation process.

Obviously the main conclusion of this work only concerns unconfined and confined simple shear flows. The analysis of more complex flows is a work in progress whose main difficulty lies in the correct definition of the appropriate flow kinematics at the RVE level.

Finally, as highlighted in the abstract and elsewhere in the paper, these conclusions rest on the validity of the considered state-of-the-art DNS, an issue that remains at present an open question and that future works should address.

References

[1] Abisset-Chavanne E, Mezher R, Le Corre S, Ammar A, Chinesta F. Kinetic theory microstructure modeling in concentrated suspensions. Entropy 2013;15:2805–32.

[2] Abisset-Chavanne E, Chinesta F, Ferec J, Ausias G, Keunings R. On the multiscale description of dilute suspensions of non-Brownian rigid clusters composed of rods. J Non-Newtonian Fluid Mech 2015;222:34–44.

[3] Binetruy C, Chinesta F, Keunings R. Flows in polymers, reinforced polymers and composites, a multiscale approach. Springerbriefs, Springer; 2015.

[4] Advani S, Tucker Ch. The use of tensors to describe and predict fibre orientation in short fibre composites. J Rheol 1987;31:751–84.

[5] Advani S, Tucker Ch. Closure approximations for three-dimensional structure tensors. J Rheol 1990;34:367–86.

[6] Ammar A, Chinesta F. A particle strategy for solving the Fokker-Planck equation governing the fibre orientation distribution in steady recirculating flows involving short fibre suspensions. Lectures notes on computational science and engineering, vol. 43. Springer; 2005. p. 1–16.

[7] Ammar A, Mokdad B, Chinesta F, Keunings R. A new family of solvers for some classes of multidimensional partial differential equations encountered in kinetic theory modeling of complex fluids. J Non-Newtonian Fluid Mech 2006;139:153–76.

[8] Ammar A, Mokdad B, Chinesta F, Keunings R. A new family of solvers for some classes of multidimensional partial differential equations encountered in kinetic theory modeling of complex fluids. Part II: Transient simulation using space-time separated representations. J Non-Newtonian Fluid Mech 2007;144:98–121.

[9] Ausias G, Fan XJ, Tanner R. Direct simulation for concentrated fibre suspensions in transient and steady state shear flows. J Non-Newtonian Fluid Mech 2006;135:46–57.

[10] Chaubal CV, Srinivasan A, Egecioglu O, Leal LG. Smoothed particle hydrodynamics techniques for the solution of kinetic theory problems. J Non-Newtonian Fluid Mech 1997;70:125–54.

[11] Chauviere C, Lozinski A. Simulation of dilute polymer solutions using a Fokker-Planck equation. Comput Fluids 2004;33:687–96.

[12] Chiba K, Ammar A, Chinesta F. On the fibre orientation in steady recirculating flows involving short fibres suspensions. Rheol Acta 2005;44:406–17.

[13] Chinesta F, Chaidron G, Poitou A. On the solution of the Fokker-Planck equation in steady recirculating flows involving short fibre suspensions. J Non-Newtonian Fluid Mech 2003;113:97–125.

[14] Chinesta F, Ammar A, Falco A, Laso M. On the reduction of stochastic kinetic theory models of complex fluids. Modell Simul Mater Sci Eng 2007;15(6):639–52.

[15] Chinesta F, Ammar A, Leygue A, Keunings R. An overview of the proper generalized decomposition with applications in computational rheology. J Non-Newtonian Fluid Mech 2011;166:578–92.

[16] Chinesta F, Keunings R, Leygue A. The proper generalized decomposition for advanced numerical simulations, a primer. Springerbriefs, Springer; 2014.

[17] Chung DH, Won TH. Improved model of orthotropic closure approximation for flow induced fiber orientation. Polym Compos 2001;22(5):636–49.

[18] Cruz C, Illoul L, Chinesta F, Regnier G. Effects of a bent structure on the linear viscoelastic response of carbon nanotube diluted suspensions. Rheol Acta 2010;49:1141–55.

[19] Cruz C, Chinesta F, Regnier G. Review on the Brownian dynamics simulation of bead-rod-spring models encountered in computational rheology. Archives Comput Methods Eng 2012;19(2):227–59.

[20] D'Avino G, Hulsen MA, Greco F, Maffettone PL. Bistability and metabistability scenario in the dynamics of an ellipsoidal particle in a sheared viscoelastic fluid. Phys Rev E 2014;89:043006.

[21] Dupret F, Verleye V. Modelling the flow of fibre suspensions in narrow gaps. In: Siginer DA, De Kee D, Chabra RP, editors. Advances in the flow and rheology of non-Newtonian fluids. Rheol Ser. Elsevier; 1999. p. 1347–98.

[22] Ferec J, Ausias G, Heuzey MC, Carreau P. Modeling fibre interactions in semiconcentrated fibre suspensions. J Rheol 2009;53(1):49–72.

[23] Ferec J, Abisset-Chavanne E, Ausias G, Chinesta F. The use of interaction tensors to describe and predict rod interactions in rod suspensions. Rheol Acta 2014;53(5–6):445–56.

[24] Folgar F, Tucker Ch. Orientation behavior of fibres in concentrated suspensions. J Reinf Plast Comp 1984;3:98–119.

[25] Grassia P, Hinch J, Nitsche LC. Computer simulations of Brownian motion of complex systems. J Fluid Mech 1995;282:373–403.

[26] Grassia P, Hinch J. Computer simulations of polymer chain relaxation via Brownian motion. J Fluid Mech 1996;308:255–88.

[27] Jackson WC, Advani SG, Tucker CL. Predicting the orientation of short fibers in thin compression moldings. J Compos Mater 1986;20(6):539–57.

[28] Jeffery GB. The motion of ellipsoidal particles immersed in a viscous fluid. Proc R Soc London 1922;A102:161–79.

[29] Kroger M, Ammar A, Chinesta F. Consistent closure schemes for statistical models of anisotropic fluids. J Non-Newtonian Fluid Mech 2008;149:40–55.

[30] Le Corre S, Caillerie D, Orgéas L, Favier D. Behavior of a net of fibres linked by viscous interactions: theory and mechanical properties. J Mech Phys Solids 2004;52(2):395–421.

[31] Le Corre S, Dumont P, Orgéas L, Favier D. Rheology of highly concentrated planar fibre suspensions. J Rheol 2005;49(5):1029.

[32] Lozinski A, Chauviere C. A fast solver for Fokker-Planck equation applied to viscoelastic flows calculations: 2D FENE model. J Comput Phys 2003;189:607–25.

[33] Ma A, Chinesta F, Ammar A, Mackley M. Rheological modelling of carbon nanotube aggregate suspensions. J Rheol 2008;52(6):1311–30.

[34] Ma A, Chinesta F, Mackley M. The rheology and modelling of chemically treated carbon nanotube suspensions. J Rheol 2009;53(3):547–73.

[35] Mezher R, Abisset-Chavanne E, Ferec J, Ausias G, Chinesta F. Direct simulation of concentrated fibre suspensions subjected to bending effects. Modell Simul Mater Sci Eng 2015;23(5):055007.

[36] Perez M, Scheuer A, Abisset-Chavanne E, Chinesta F, Keunings R. A multi-scale description of orientation in confined suspensions involving rods. J Non-Newtonian Fluid Mech 2016;233:61–74. doi: http://dx.doi.org/10.1016/j.jnnfm.2016.01.011.

[37] Phelps J, Tucker Ch. An anisotropic rotary diffusion model for fibre orientation in short and long fibre thermoplastics. J Non-Newtonian Fluid Mech 2009;156(3):165–76.

[38] Pruliere E, Ammar A, El Kissi N, Chinesta F. Recirculating flows involving short fibre suspensions: numerical difficulties and efficient advanced micro-macro solvers. Archives Comput Methods Eng State Art Rev 2009;16:1–30.

[39] Wang J, Silva CA, Viana JC, van Hattum FWJ, Cunha AM, Tucker Ch. Prediction of fibre orientation in a rotating compressing and expanding mold. Polym Eng Sci 2008:1405–13.

[40] Wang J, O'Gara J, Tucker Ch. An objective model for slow orientation kinetics in concentrated fibre suspensions: theory and rheological evidence. J Rheol 2008;52(5):1179–200.